

## Supporting Information

### "Ethanol-Water Exchange" Nanobubbles Templated Hierarchical Hollow $\beta$ -Mo<sub>2</sub>C/N-doped Carbon Nanospheres as an Efficient Hydrogen Evolution Electrocatalyst

Lechen Diao <sup>a</sup>, Jian Qin <sup>a</sup>, Naiqin Zhao <sup>a, b, c</sup>, Chunsheng Shi <sup>a</sup>, Enzuo Liu <sup>a,b</sup>, Fang He <sup>a</sup>,

Liyang Ma <sup>a</sup>, Jiajun Li <sup>a</sup>, Chunlian He\*, <sup>a, b, c</sup>

<sup>a</sup> School of Materials Science and Engineering and Tianjin Key Laboratory of Composites and Functional Materials, Tianjin University, Tianjin, 300072, P. R. China

<sup>b</sup> Collaborative Innovation Center of Chemical Science and Engineering, Tianjin 300072, China

<sup>c</sup> Key Laboratory of Advanced Ceramics and Machining Technology, Ministry of Education, Tianjin University, Tianjin 300072, China

Corresponding Authors

\* E-mail: cnhe08@tju.edu.cn (C. He).

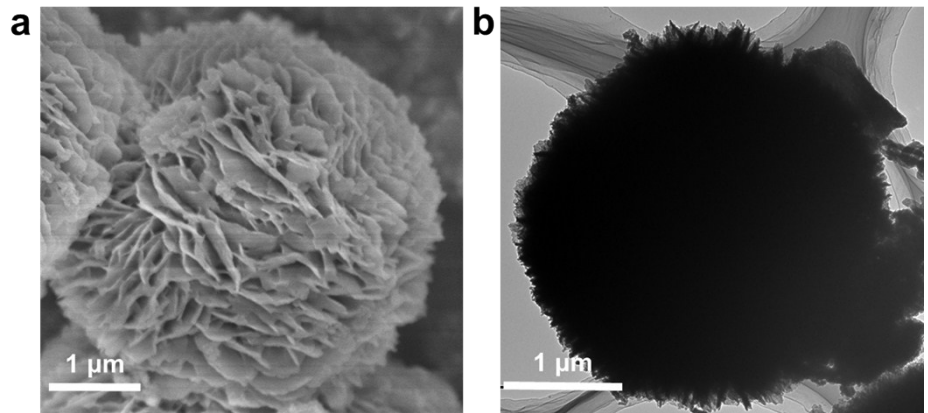


**Fig. S1.** FESEM (a) and TEM (b) images of the solid spheres produced when ethanol was replaced by an equal volume of water.

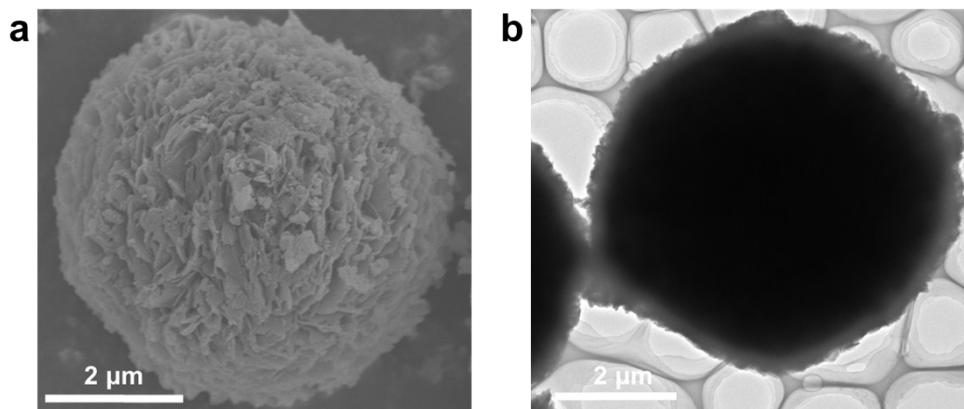


**Fig. S2.** FESEM (a) and TEM (b) images of the obtained solid spheres consisting of nanosheets produced when ethanol was reduced to 30 mL.

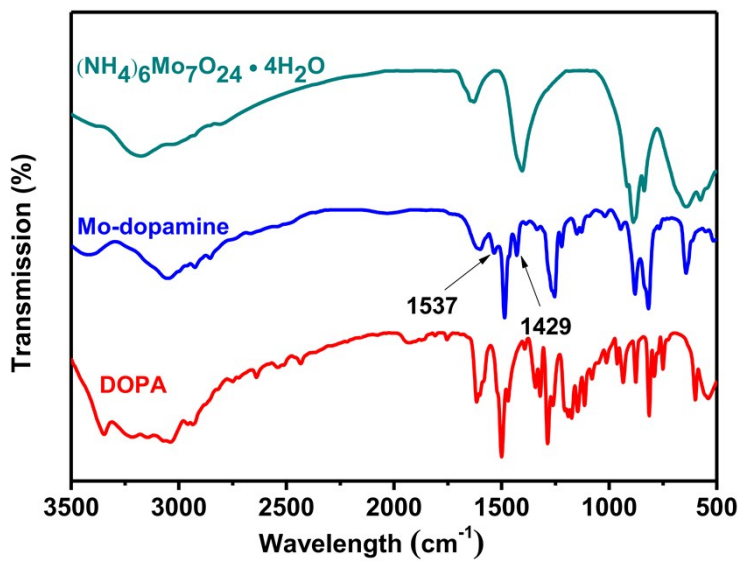


**Fig. S3.** FTIR spectra of dopamine, Mo-dopamine and  $(\text{NH}_4)_6\text{Mo}_7\text{O}_{24} \cdot 4\text{H}_2\text{O}$ .

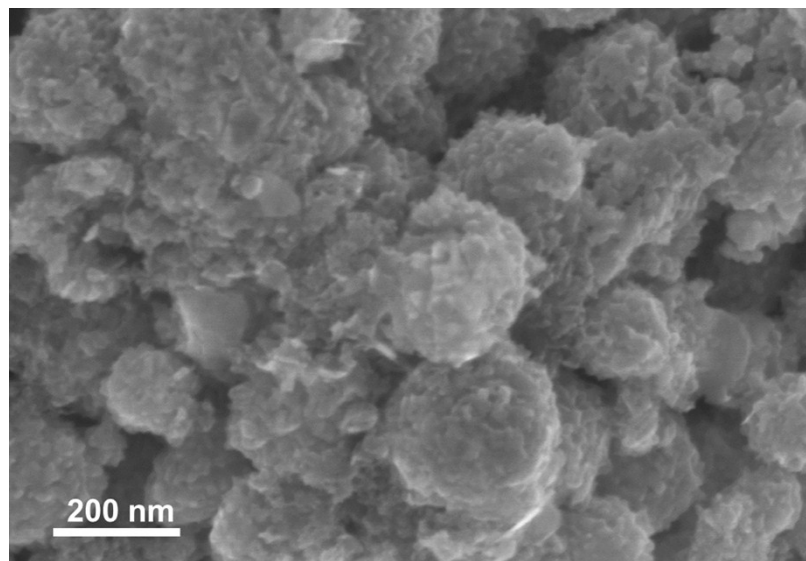


**Fig. S4.** SEM image of the product extracted from the system at 5 min through high-temperature treatment.

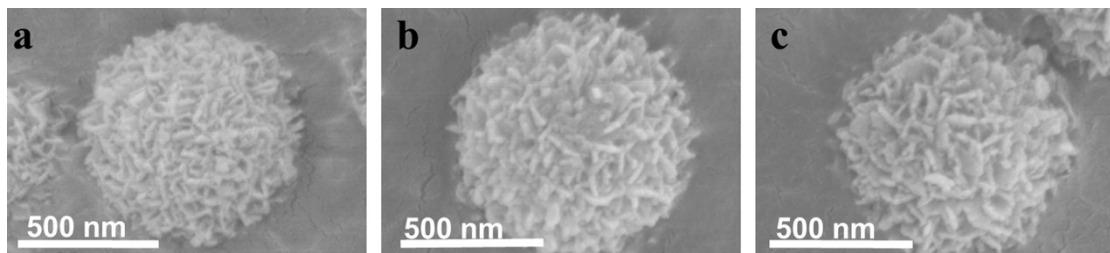


**Fig. S5.** SEM image of the product extracted from the system at a) 5 min, b) 1 h, and c) 2 h.

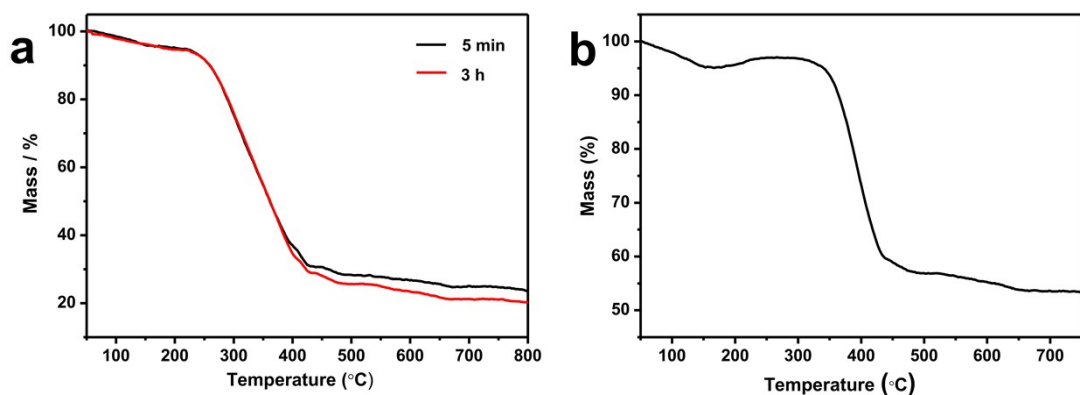


**Fig. S6.** TGA curve of a) Mo-dopamine complex precursor at different time and b) hollow  $\beta$ -Mo<sub>2</sub>C/N-doped carbon composite nanospheres in air with a heating rate of  $10\text{ }^{\circ}\text{C}\cdot\text{min}^{-1}$ .

$$m_{(\text{Mo}_2\text{C})} = w_{(\text{MoO}_3)} \times M_{(\text{Mo}_2\text{C})} / 2M_{(\text{MoO}_3)} = 53.3\% \times 204 / (2 \times 144) = 37.8\%.$$

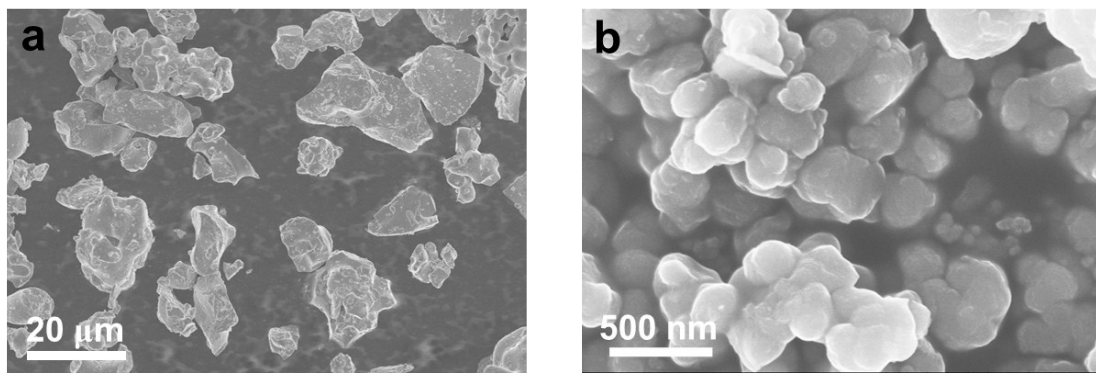


**Fig. S7.** SEM images of a) commercial  $\beta$ -Mo<sub>2</sub>C, and b) N-doped carbon.

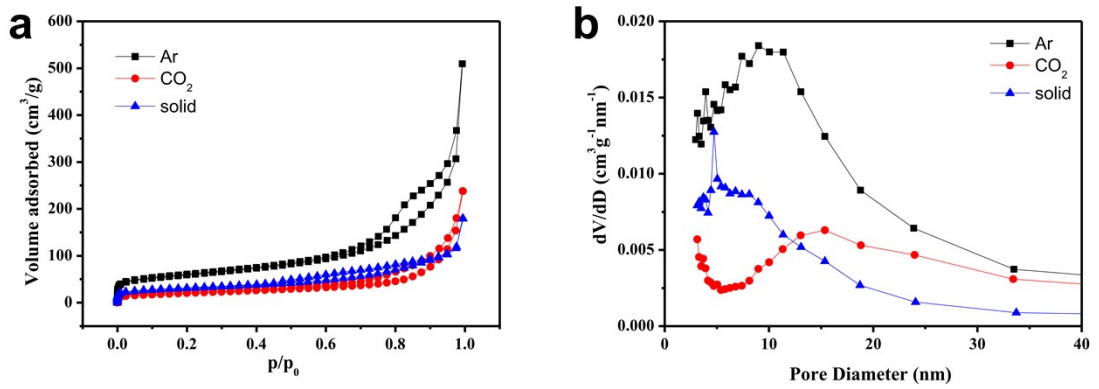


**Fig. S8.** a) Nitrogen adsorption-desorption isotherm of  $\beta\text{-Mo}_2\text{C}$  nanoflowers at 77 K, and b) the corresponding pore size distribution derived from the adsorption branches on the basis of the BJH model.

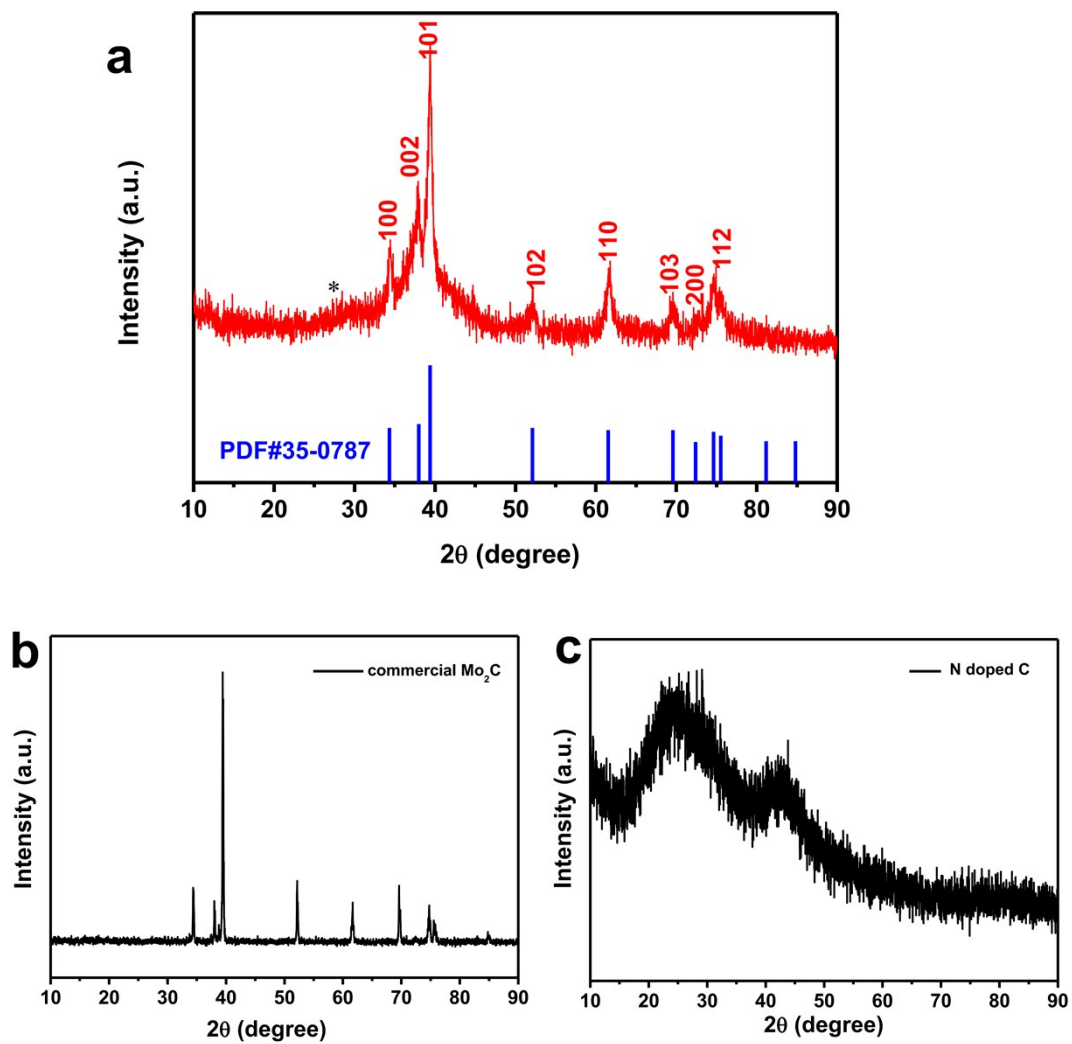


**Fig. S9.** XRD of the a) hollow  $\beta$ - $\text{Mo}_2\text{C}$ /N-doped carbon composite nanospheres, b) commercial  $\beta$ - $\text{Mo}_2\text{C}$ , and c) N-doped carbon.

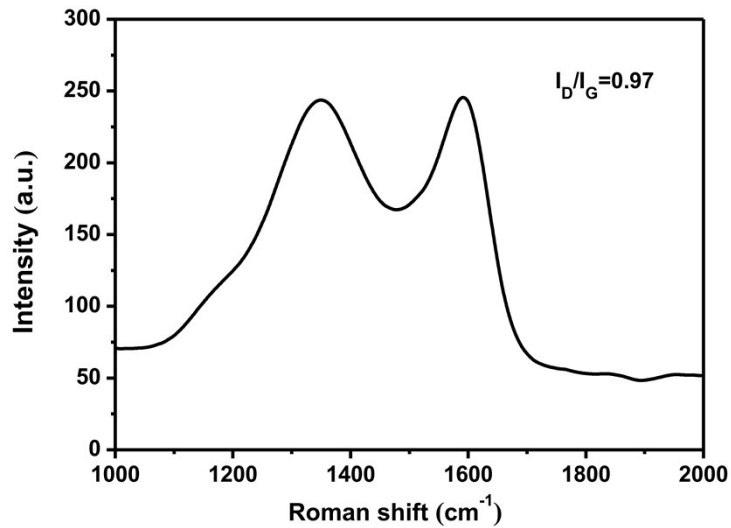


**Fig. S10.** Raman spectra of the hollow  $\beta\text{-Mo}_2\text{C}/\text{N}$ -doped carbon composite nanospheres.

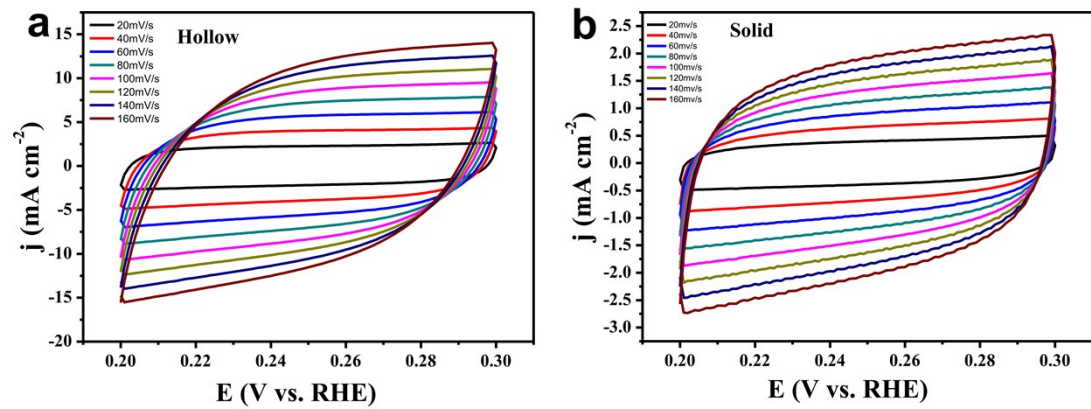


**Fig. S11.** Cyclic voltammograms in the region of 0.2–0.3 V vs. RHE for a) the hollow  $\beta\text{-Mo}_2\text{C}/\text{N}$ -doped carbon composite nanospheres and b) the solid  $\beta\text{-Mo}_2\text{C}/\text{N}$ -doped carbon composite spheres.

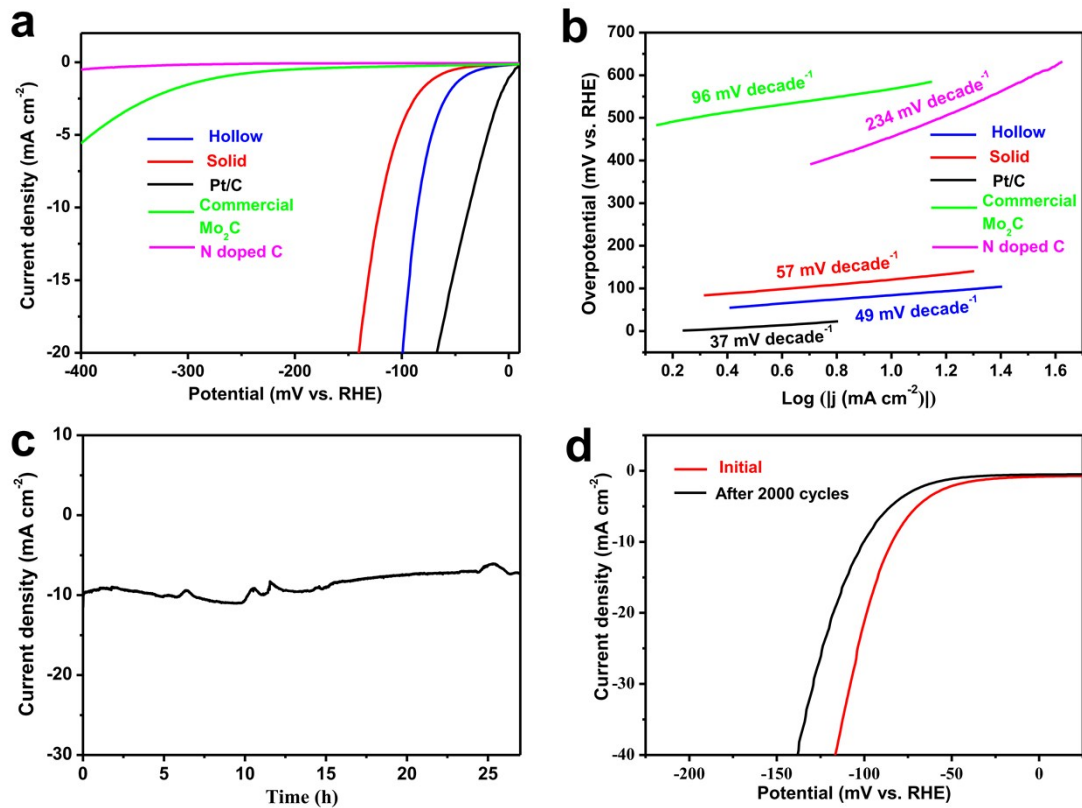


**Fig. S12.** HER tests in 1 M KOH. a) The HER polarization plots for different catalysts at a scan rate of  $5 \text{ mV s}^{-1}$ , b) Tafel plots for different catalysts, c) The i-t curve at  $\eta=130 \text{ mV}$ , d) Polarization curves of the hollow  $\beta$ -Mo<sub>2</sub>C/N-doped carbon composite nanospheres before and after 2000 CV scans .

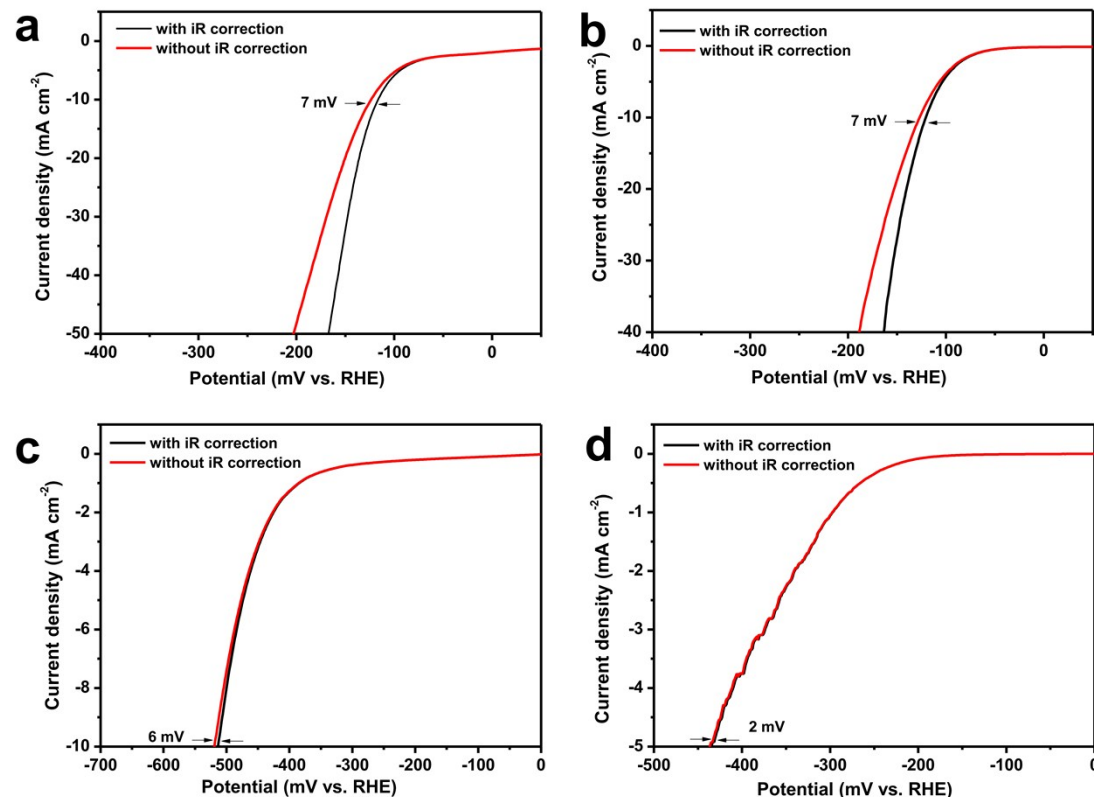


**Fig. S13.** The LSV curves before and after iR correction in 0.5 M H<sub>2</sub>SO<sub>4</sub>. a) hollow β-Mo<sub>2</sub>C nanoflowers, b) β-Mo<sub>2</sub>C nanoflowers, c) N doped carbon, and d) commercial β-Mo<sub>2</sub>C nanoflowers.

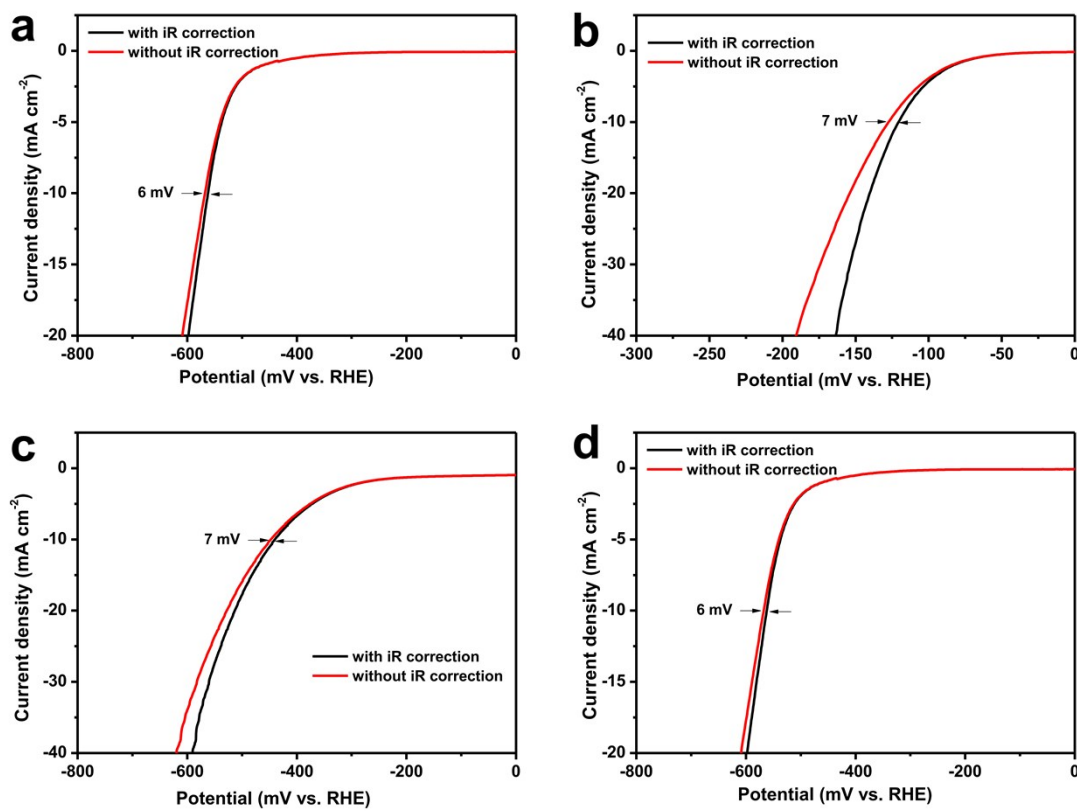


**Fig. S14.** The LSV curves before and after iR correction in 1 M KOH. a) hollow β-Mo<sub>2</sub>C nanoflowers, b) β-Mo<sub>2</sub>C nanoflowers, c) N doped carbon, and d) commercial β-Mo<sub>2</sub>C nanoflowers.

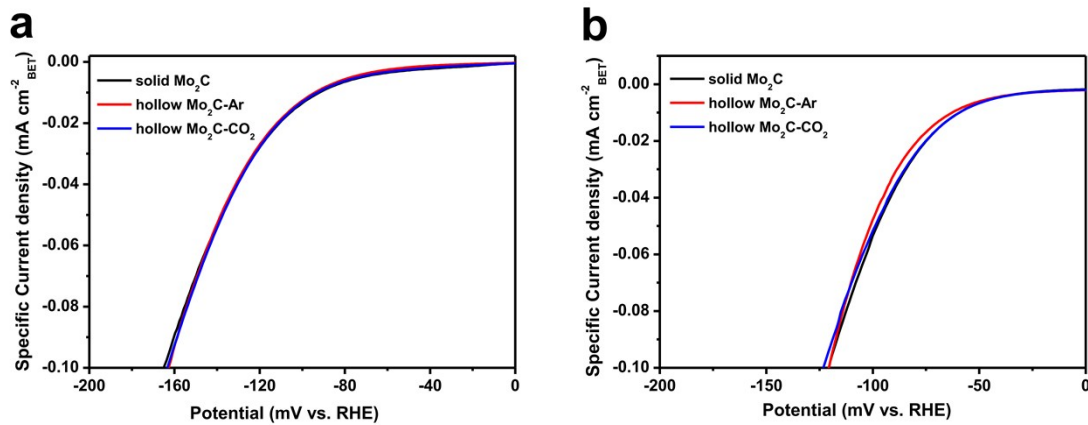


**Fig. S15.** Polarization curves normalized by the BET a) 0.5 M H<sub>2</sub>SO<sub>4</sub>, and b) 1 M KOH.

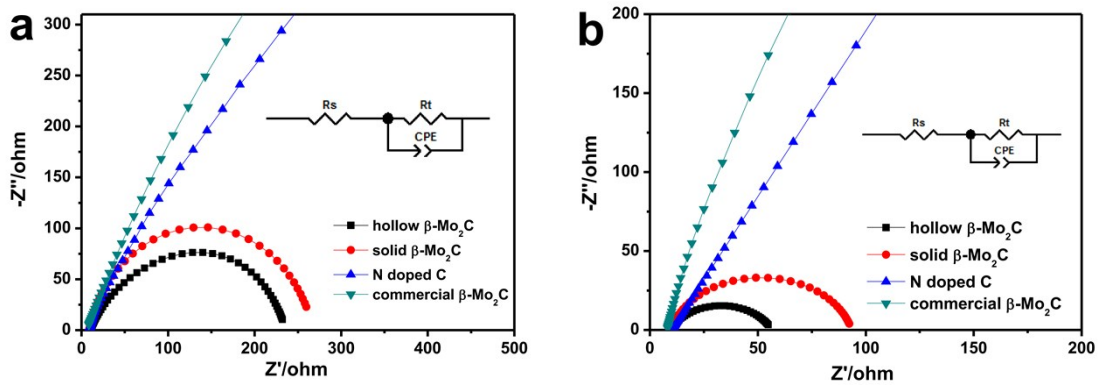


**Fig. S16.** ESI spectra for hollow and solid  $\beta\text{-Mo}_2\text{C}$ . a) 0.5 M  $\text{H}_2\text{SO}_4$ , and b) 1 M KOH.

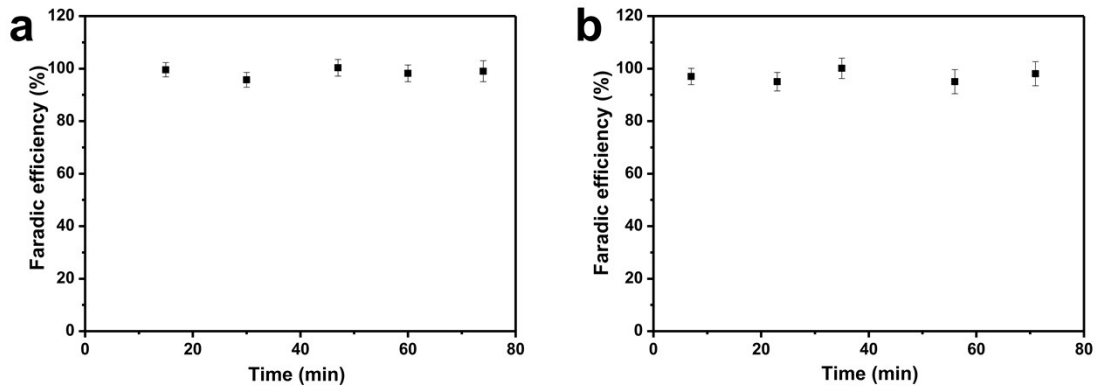


**Fig. S17.** Faradaic efficiency of the hollow  $\beta\text{-Mo}_2\text{C}/\text{N-doped carbon composite}$  nanospheres from gas chromatography measurement of evolved  $\text{H}_2$  to within our available  $\pm 5\%$  experimental error. a) 0.5M  $\text{H}_2\text{SO}_4$ , and b) 1M KOH.

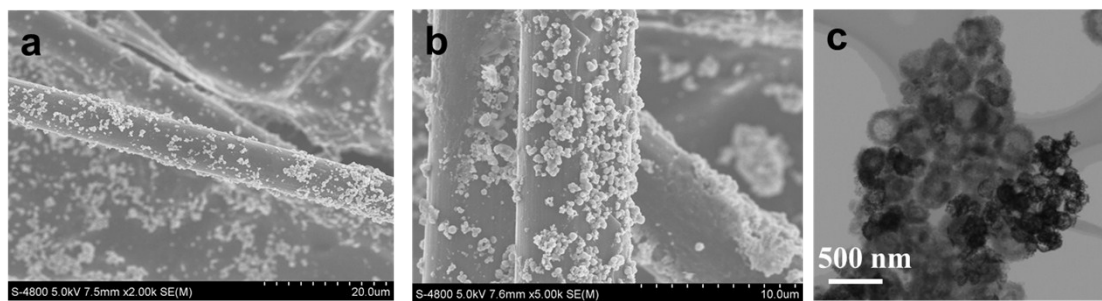


**Fig. S18.** FESEM (a,b) and TEM (c) images of the hollow  $\beta\text{-Mo}_2\text{C}$  nanoflowers deposited in carbon fiber paper. (a) before i-t, (b,c) after i-t.

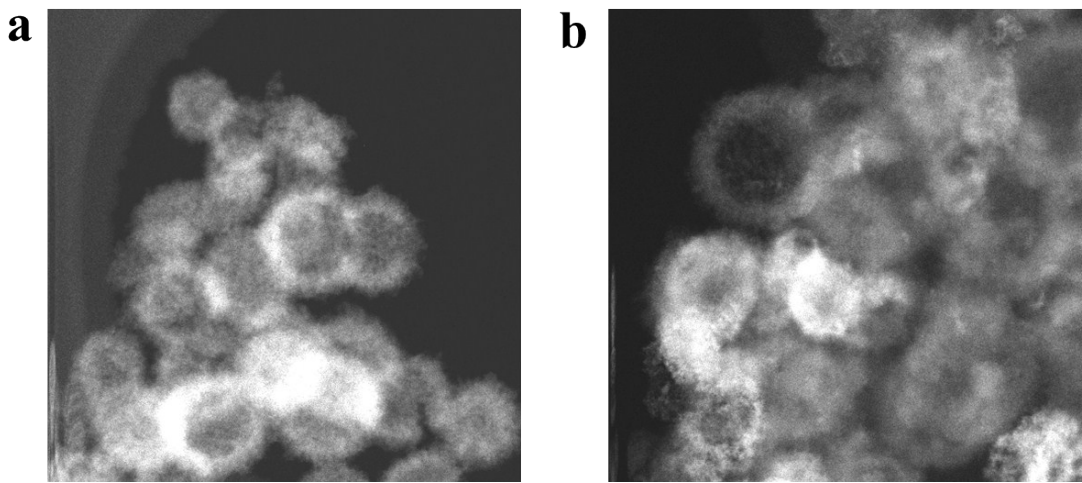


**Fig. S19.** HAADF-STEM of hollow  $\beta$ -Mo<sub>2</sub>C nanoflowers. a) before i-t test and b) after i-t test in 1 M KOH.

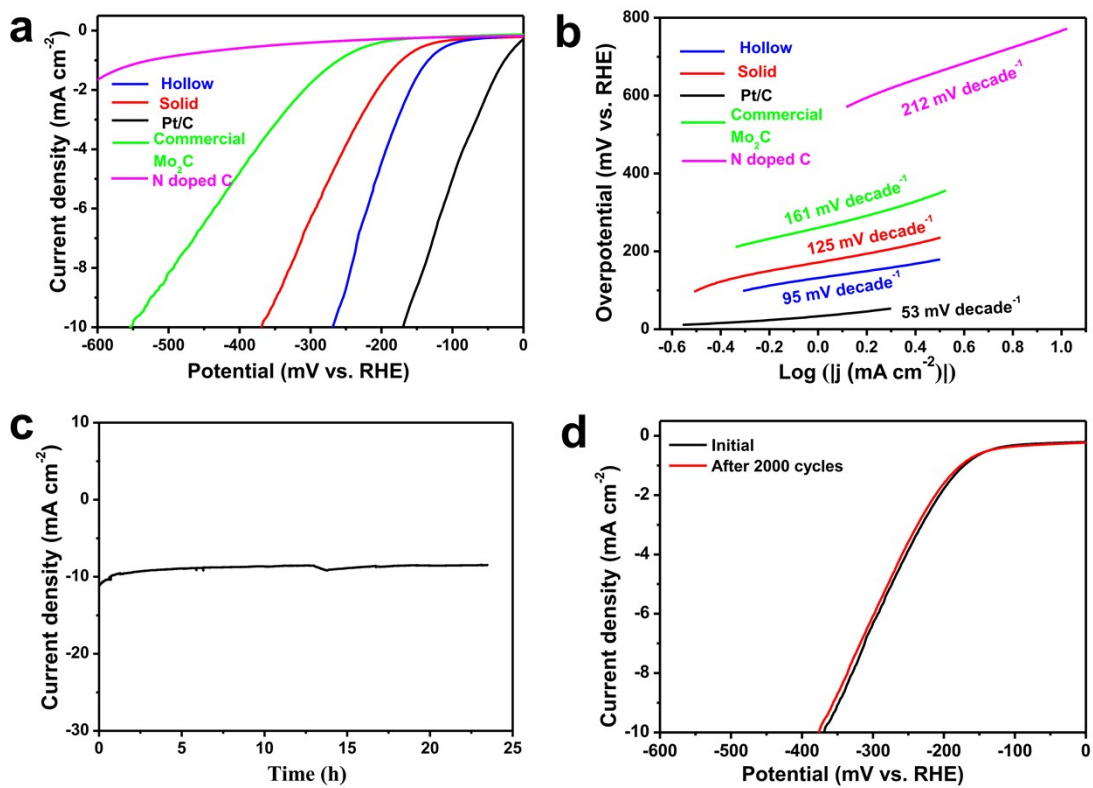


**Fig. S20.** HER tests in 1 M PBS. a) The HER polarization plots for different catalysts at a scan rate of 5 mV s<sup>-1</sup>, b) Tafel plots for different catalysts, c) the i-t curve at  $\eta=320$  mV, and d) polarization curves of the hollow  $\beta$ -Mo<sub>2</sub>C nanoflowers before and after 2000 CV scans .

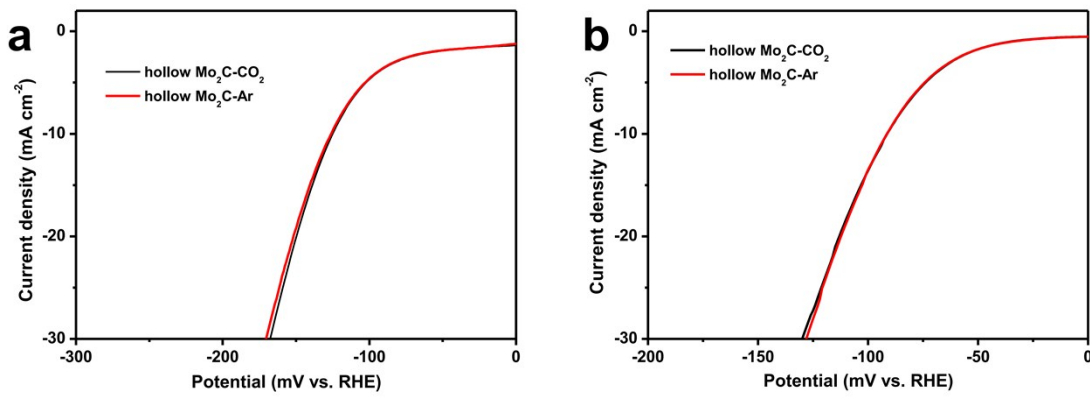


**Fig. S21.** Polarization curves of the hollow  $\beta$ - $\text{Mo}_2\text{C}-\text{CO}_2$  and  $\beta$ - $\text{Mo}_2\text{C}-\text{Ar}$ . a) 0.5 M  $\text{H}_2\text{SO}_4$ , and b) 1 M KOH.

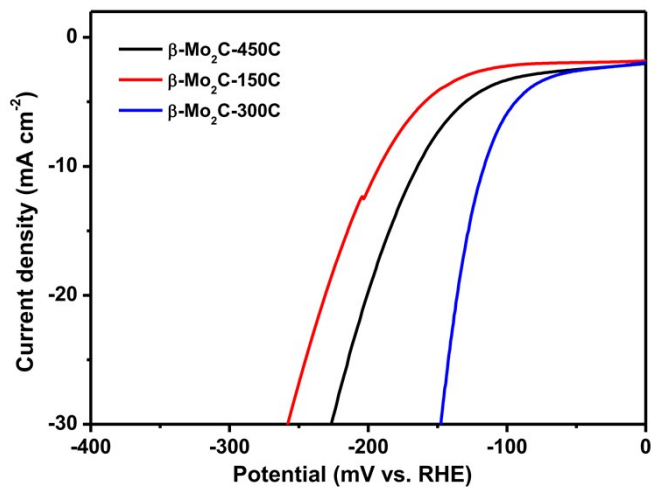


**Fig. S22.** Polarization curves of the hollow  $\beta$ - $\text{Mo}_2\text{C}-150\text{C}$ ,  $\beta$ - $\text{Mo}_2\text{C}-300\text{C}$  and  $\beta$ - $\text{Mo}_2\text{C}-450\text{C}$  in 0.5 M  $\text{H}_2\text{SO}_4$ .

**Table S1.** Relative atomic ratio of the hollow  $\beta$ - $\text{Mo}_2\text{C}/\text{N}$ -doped carbon composite nanospheres from XPS analysis.

element	C1s	N1s	O1s	Mo3d
Relative atomic ratio (atm.%)	51.85	16	21.09	11.07
Binding energy (eV)	284.80	398.80	530.89	228.84 232.77

**Table S2. Surface area and pore diameter of the sample.**

sample	Surface area ( $\text{m}^2 \text{ g}^{-1}$ )	Pore Diameter (nm)
$\beta\text{-Mo}_2\text{C-Ar}$	71.7	9.0
$\beta\text{-Mo}_2\text{C-CO}_2$	73.4	15.3
Solid $\beta\text{-Mo}_2\text{C}$	25.4	4.7

**Table S3.** Comparison of the HER activity in acidic electrolyte of the hollow  $\beta\text{-Mo}_2\text{C}$ /N-doped carbon composite nanospheres and other  $\text{Mo}_2\text{C}$  based electrocatalysts reported in literature.

Catalyst	Current density ( $\text{j, mA cm}^{-2}$ )	electrolyte	$\eta$ at the correspondin g $\text{j}$ (mV)	Tafel slope (mV/dec)	Reference
<b>pomegranate-like <math>\text{Mo}_2\text{C@C}</math> nanospheres</b>	10	0.5M $\text{H}_2\text{SO}_4$	141	56	ACS Nano 2016, 10, 8851
<b><math>\text{Mo}_2\text{C QD/NGCL}</math></b>	10	0.5M $\text{H}_2\text{SO}_4$	136	68.4	Chem. Commun., 2016, 52, 12753
<b><math>\text{Mo}_2\text{C@NC}</math></b>	10	0.5M $\text{H}_2\text{SO}_4$	124	60	Angew. Chem. Int. Ed. 2015, 54, 10752
<b><math>\text{Mo}_2\text{C}</math> on carbon cloth</b>	10	0.5M $\text{H}_2\text{SO}_4$	140	124	J. Mater. Chem. A, 2015, 3, 16320
<b><math>\beta\text{-Mo}_2\text{C}</math> nanoparticles</b>	10	0.5M $\text{H}_2\text{SO}_4$	165	55	Journal of Power Sources 2015, 296, 18-22
<b><math>\text{Mo}_2\text{C-N}</math> doped CNT</b>	10	0.5M $\text{H}_2\text{SO}_4$	147	71	J. Mater. Chem. A, 2015, 3, 5783
<b><math>\text{MoCx}</math> nano- octahedrons</b>	10	0.5M $\text{H}_2\text{SO}_4$	142	53	DOI: 10.1038/ncomms7512
<b><math>\text{Mo}_2\text{C}</math></b>	10	0.5M $\text{H}_2\text{SO}_4$	198	56	J. Mater. Chem. A, 2015, 3, 8361
<b><math>\text{MoC-Mo}_2\text{C}</math> heteronanowires</b>	10	0.5M $\text{H}_2\text{SO}_4$	126	43	Chem. Sci., 2016, 7, 3399
<b><math>\text{MoSoy}</math></b>	10	0.1 M $\text{HClO}_4$	177		Energy Environ. Sci., 2013, 6, 1818

<b>Mo<sub>2</sub>C-C</b>	10	0.5M H <sub>2</sub> SO <sub>4</sub>	164	85	Nano Energy 2017, 32, 511–519
<b>Mo<sub>2</sub>C/C microflowers</b>	10	0.5M H <sub>2</sub> SO <sub>4</sub>	146	60	Adv. Energy Mater. 2017, 1602782
<b>P doped Mo<sub>2</sub>C@C nw</b>	10	0.5M H <sub>2</sub> SO <sub>4</sub>	89	42	Energy Environ. Sci., 2017, 10, 1262--1271
<b>Hollow β-Mo<sub>2</sub>C/N-doped carbon composite nanospheres</b>	<b>10</b>	<b>0.5M H<sub>2</sub>SO<sub>4</sub></b>	<b>119</b>	<b>67</b>	<b>This work</b>

**Table S4.** Comparison of the HER activity in alkaline electrolyte of the hollow β-Mo<sub>2</sub>C/N-doped carbon composite nanospheres and other Mo<sub>2</sub>C based electrocatalysts reported in literature.

Catalyst	Current density (j, mA cm <sup>-2</sup> )	electrolyt e	η at the corresponding j (mV)	Tafel slope (mV/dec)	Reference
<b>pomegranate-like Mo<sub>2</sub>C@C nanospheres</b>	10	1M KOH	47	71	ACS Nano 2016, 10, 8851
<b>Mo<sub>2</sub>C QD/NGCL</b>	10	1M KOH	111	57.8	Chem. Commun., 2016, 52, 12753
<b>Mo<sub>2</sub>C@NC</b>	10	1M KOH	60		Angew. Chem. Int. Ed. 2015, 54, 10752
<b>(Mo<sub>2</sub>C)<sub>0.34</sub>-(WC)<sub>0.32</sub>/NG</b>	10	1M KOH	93	53	DOI: 10.1039/c7ta02864d
<b>Mo<sub>2</sub>C@NPC</b>	10	1M NaOH	141	47.5	J. Mater. Chem. A, 2017, 5, 5178
<b>NiMo<sub>2</sub>C@C</b>	10	1M KOH	181	84	J. Mater. Chem. A, 2017, 5, 5000
<b>MoCx nano-octahedrons</b>	10	1M KOH	151	59	DOI: 10.1038/ncomms7512
<b>Mo<sub>2</sub>C</b>	10	1M KOH	176	58	J. Mater. Chem. A, 2015, 3, 8361
<b>MoC-Mo<sub>2</sub>C heteronanowires</b>	10	1M KOH	120	42	Chem. Sci., 2016, 7, 3399
<b>Mo<sub>2</sub>C</b>	10	1M KOH	96	62.2	J. Mater. Chem. A, 2017, 5, 4879

<b>Mo<sub>2</sub>C-C</b>	10	1M KOH	149	66	Nano Energy 2017, 32, 511–519
<b>Mo<sub>2</sub>C/C microflowers</b>	10	1M KOH	140	58	Adv. Energy Mater. 2017, 1602782
<b>Hollow β-Mo<sub>2</sub>C/N-doped carbon composite nanospheres</b>	<b>10</b>	<b>1M KOH</b>	<b>85</b>	<b>49</b>	<b>This work</b>

**Table S5.** The charge transfer resistance of different samples measured in 0.5 M H<sub>2</sub>SO<sub>4</sub>.

Simple(H <sub>2</sub> SO <sub>4</sub> )	Rs(Ω)	Rt(Ω)
<b>Hollow β-Mo<sub>2</sub>C</b>	10.23	226
<b>solid β-Mo<sub>2</sub>C</b>	9.05	258.6
<b>N doped C</b>	8.05	1761
<b>Commercial β-Mo<sub>2</sub>C</b>	5.80	2818

**Table S6.** The charge transfer resistance of different samples measured in 1 M KOH.

Simple(KOH)	Rs(Ω)	Rt(Ω)
<b>Hollow β-Mo<sub>2</sub>C</b>	9.39	61.43
<b>solid β-Mo<sub>2</sub>C</b>	9.74	90.68
<b>N doped C</b>	10.47	3178
<b>Commercial β-Mo<sub>2</sub>C</b>	7.92	3366

**Table S7.** The concentrations of Mo measured by ICP-AES after HER in both 0.5 M H<sub>2</sub>SO<sub>4</sub> and 1 M KOH.

Electrolyte sample	Concentrations of Mo in electrolyte (ppm)
<b>0.5 M H<sub>2</sub>SO<sub>4</sub></b>	0.22
<b>1 M KOH</b>	1

**Table S8.** Comparison of the HER activity in neutral electrolyte of the hollow  $\beta$ -Mo<sub>2</sub>C/N-doped carbon composite nanospheres and other electrocatalysts reported in literature.

Catalyst	Current density (j, mA cm <sup>-2</sup> )	electrolyte	$\eta$ at the corresponding j (mV)	Tafel slope (mV/dec)	Reference
<b>CoMoS<sub>4</sub> NTA/CC</b>	10	1M PBS	179	77	Chemistry-A European Journal, 2017, 23, 12718-12723
<b>CoP NA/CC</b>	10	1M PBS	145	123	ChemElectroChem, 2017, 4, 1840-1845
<b>CoP/CC</b>	2	1M PBS	65	93	J. Am. Chem. Soc. 2014, 136, 7587–7590
<b>FeMoS<sub>4</sub> NRA/CC</b>	10	1M PBS	204	128	Chem. Commun., 2017, 53, 9000--9003
<b>Co<sub>2</sub>N/TM</b>	10	1M PBS	290	138	Catal. Sci. Technol., 2017, 7, 2689–2694
<b>Co-NRCNTs/GCE</b>	10	1M PBS	540		Angew. Chem. 2014, 126, 4461 –4465
<b>CoO/CoSe<sub>2</sub>/Ti</b>	10	0.5M PBS	337	131	Adv.Sci.2016, 3, 1500426
<b>WN NAs/CC</b>	10	1M PBS	302	182	Electrochimica Acta 154 (2015) 345–351
<b>Cu-EA</b>	2	0.1M PBS	270		Chem. Commun., 2015, 51, 12954-12957
<b>cobalt @ cobalt-oxo / hydroxo phosphate</b>	2	0.5M phosphate buffer (KPi, pH = 7)	385		Nat. Mater. 2012, 11, 802

					Angew. Chem.
<b>Mo<sub>2</sub>C</b>	1	1M PBS	200		Int. Ed. 2012,
<b>Hollow β-Mo<sub>2</sub>C/N-</b>					51, 12703
<b>doped carbon</b>	<b>10</b>	<b>1M PBS</b>	<b>268</b>	<b>95</b>	<b>This work</b>
<b>composite nanospheres</b>					

---